Decay Constants of B and D Mesons from Non-perturbatively Improved Lattice QCD

UKQCD Collaboration

K.C. Bowler [a], L. Del Debbio [b,1], J.M. Flynn [b],
G.N. Lacagnina [a], V.I. Lesk [b], C.M. Maynard [a],
D.G. Richards [a,c,d]

[a] *Department of Physics & Astronomy, University of Edinburgh, Edinburgh EH9 3JZ, Scotland, UK*

[b] *Department of Physics & Astronomy, University of Southampton, Southampton, SO17 1BJ, UK*

[c] *Jefferson Laboratory, MS 12H2, 12000 Jefferson Avenue, Newport News, VA 23606, USA.*

[d] *Department of Physics, Old Dominion University, Norfolk, VA 23529, USA.*

Abstract

The decay constants of B and D mesons are computed in quenched lattice QCD at two different values of the coupling. The action and operators are $\mathcal{O}(a)$ improved with non-perturbative coefficients where available. The results are $f_{\mathrm{B}} = 218^{+5+\ 5}_{-5-41}$ MeV, $f_{\mathrm{D}} = 220^{+3+\ 2}_{-3-24}$ MeV, $f_{\mathrm{B_s}} = 242^{+4+13}_{-4-48}$ MeV, $f_{\mathrm{D_s}} = 241^{+2+\ 7}_{-2-30}$ MeV. Systematic errors are discussed in detail. Results for vector decay constants, flavour symmetry breaking ratios of decay constants, the pseudoscalar-vector mass splitting and D meson masses are also presented.

PACS numbers:12.38Gc, 13.20Fc, 13.20Hc, 14.40Lb, 14.40Nd

[1] Dipartimento di Fisica, Università di Pisa and INFN Sezione di Pisa, Italy.

arXiv:hep-lat/0007020 v2   17 Jul 2000

1 Introduction

The accurate determination of the B and D meson decay constants is of vital importance in phenomenology. The combination $f_B\sqrt{B_B}$, for both B_d and B_s mesons, plays a crucial role in the extraction from experimental data of CKM quark mixing and CP violation parameters. The phenomenological parameter B_B describes B^0–$\bar{B}^0$ mixing, and is expected to be close to unity. D meson decay constants are needed for calculations based on factorisation of non-leptonic B meson decays to charmed mesons (see [1] for a review and [2] for a recent application).

This paper presents decay constants and masses of heavy-light mesons calculated in the quenched approximation to QCD, at two values of the lattice coupling, $\beta = 6.2$ and $\beta = 6.0$. Using a non-perturbatively improved SW fermion action and improved operators makes the leading discretisation errors in lattice matrix elements appear at $\mathcal{O}(a^2)$ rather than $\mathcal{O}(a)$, but does not imply that lattice artefacts are necessarily smaller at a given β. With results at two values of β, this issue can be partially addressed, although a continuum extrapolation is not attempted. Details of the lattice calculation and the extraction of decay constants and masses from Euclidean Green functions are described in Section 2.

The pseudoscalar and vector decay constants are related by heavy quark symmetry (HQS) in the infinite quark mass limit. Heavy quark effective theory ideas determine the heavy quark (or heavy meson) mass dependence of the decay constants, allowing an extrapolation of the lattice calculations to the B mass. The possibility of spurious heavy mass dependence arising from lattice discretisation errors must be examined. The extrapolations to physical quark masses, both heavy and light, are discussed in Section 3.

Results for the decay constants are presented in Section 4 and summarised here:

$$f_B = 218 \pm 5^{+5}_{-41} \text{ MeV} \qquad f_{B^*} = 22.6 \pm 0.7^{+4.4}_{-3.6}$$

$$f_D = 220 \pm 3^{+2}_{-24} \text{ MeV} \qquad f_{D^*} = 7.5 \pm 0.1^{+1.3}_{-0.8}$$

$$f_{B_S} = 242 \pm 4^{+13}_{-48} \text{ MeV} \qquad f_{B_s^*} = 20.9 \pm 0.4^{+3.3}_{-4.2}$$

$$f_{D_S} = 241 \pm 2^{+7}_{-30} \text{ MeV} \qquad f_{D_s^*} = 7.3 \pm 0.1^{+0.9}_{-0.4}$$

$$f_{B_s}/f_B = 1.11 \pm 0.01^{+0.05}_{-0.03} \qquad f_{B_s^*}/f_{B^*} = 0.92 \pm 0.01^{+0.04}_{-0.03}$$

$$f_{D_s}/f_D = 1.09 \pm 0.01^{+0.05}_{-0.02} \qquad f_{D_s^*}/f_{D^*} = 0.98 \pm 0.01^{+0.02}_{-0.04}$$

The first error is statistical and the second is systematic. Lattice simulations provide non-perturbative determinations of physical quantities from first prin-

ciples which are systematically improvable. Estimating the uncertainty in such physical quantities is indispensable for phenomenological applications of lattice QCD. A full analysis of systematic errors is included with the discussion of results. The major systematic variations are shown in Table 8.

2 Details of the Calculation

2.1 Improved Action and Operators

In the Wilson formulation of lattice QCD, the fermionic part of the action has lattice artifacts of $\mathcal{O}(a)$ (where a is the lattice spacing), while the gauge action differs from the continuum Yang-Mills action by terms of $\mathcal{O}(a^2)$. To leading order in a the Symanzik improvement programme involves adding the Sheikholeslami-Wohlert term [3] to the fermionic Wilson action,

$$S_{\text{SW}} = S_{\text{W}} - c_{\text{SW}} \frac{i\kappa}{2} \sum_x \bar{\psi}(x) i\sigma_{\mu\nu} F_{\mu\nu}(x) \psi(x) \tag{1}$$

The coefficient c_{SW} has been determined non-perturbatively (NP) by the ALPHA collaboration [4,5]. Full $\mathcal{O}(a)$ improvement of on-shell matrix elements also requires that the currents are suitably improved. The improved vector and axial currents are

$$V^{\text{I}}_\mu(x) = V_\mu(x) + ac_{\text{V}} \tilde{\partial}_\nu T_{\mu\nu}(x)$$
$$A^{\text{I}}_\mu(x) = A_\mu(x) + ac_{\text{A}} \tilde{\partial}_\mu P(x) \tag{2}$$

where

$$V_\mu(x) = \bar{\psi}(x)\gamma_\mu \psi(x)$$
$$A_\mu(x) = \bar{\psi}(x)\gamma_\mu \gamma_5 \psi(x)$$
$$P(x) = \bar{\psi}(x)\gamma_5 \psi(x)$$
$$T_{\mu\nu}(x) = \bar{\psi}(x)i\sigma_{\mu\nu}\psi(x)$$

and $\tilde{\partial}_\mu$ is the symmetric lattice derivative. The generic current renormalisation is as follows ($J = A, V$):

$$J^{\text{R}} = Z^J(1 + b_J am_q)J^{\text{I}} \tag{3}$$

where Z^J is calculated in a mass-independent renormalisation scheme.

The bare quark mass, am_q, is

$$am_q = \frac{1}{2}\left(\frac{1}{\kappa} - \frac{1}{\kappa_{\text{crit}}}\right) \qquad (4)$$

where κ is the hopping parameter. For non-degenerate currents, an effective quark mass is used in the definition of the renormalised current, corresponding to

$$\frac{1}{\kappa_{\text{eff}}} = \frac{1}{2}\left(\frac{1}{\kappa_1} + \frac{1}{\kappa_2}\right) \qquad (5)$$

In this renormalisation scheme, the improved quark mass, used in the chiral extrapolations, is defined as

$$\widetilde{m}_q = m_q(1 + b_{\text{m}}am_q) \qquad (6)$$

2.2 Definitions of Mesonic Decay Constants

The pseudoscalar and vector meson decay constants, f_P and f_V, are defined by

$$\langle 0|A_\mu^{\text{R}}(0)|\text{P}\rangle = ip_\mu f_P, \qquad (7)$$

$$\langle 0|V_\mu^{\text{R}}(0)|\text{V}\rangle = i\epsilon_\mu \frac{M_V^2}{f_V} \qquad (8)$$

where $|\text{P}\rangle$ is a pseudoscalar meson state with momentum p_μ, while $|\text{V}\rangle$ is a vector meson, with mass aM_V and polarisation vector ϵ_μ. A_μ^{R} (V_μ^{R}) denotes the renormalised axial (vector) current, here taken to be the renormalised, improved local lattice axial (vector) current, defined via equation (3).

2.3 Simulation Details

In this study, gauge field configurations are generated using a combination of the over-relaxed [6,7] and the Cabibbo-Marinari [8] algorithms with periodic boundary conditions at two values of the gauge coupling $\beta = 6/g_0^2$. At each β, heavy quark propagators are computed at four values of the hopping parameter, corresponding to quarks with masses in the region of the charm quark mass. For light quark propagators, three values of κ are used, corresponding to masses around that of the strange quark. Table 1 lists the input parameters. Statistical errors are estimated using the bootstrap [10] with 1000

Table 1

Input and derived parameters. The lattice spacing is set by r_0. The hopping parameters κ_{crit}, κ_{n} and κ_{s} are defined below and are taken from [9].

	$\beta = 6.2$	$\beta = 6.0$
Volume	$24^3 \times 48$	$16^3 \times 48$
c_{SW}	1.614	1.769
N_{configs}	216	305
$a^{-1}\,(\mathrm{MeV})$	2913(10)	2119(7)
Heavy κ	$0.1200, 0.1233, 0.1266, 0.1299$	$0.1123, 0.1173, 0.1223, 0.1273$
Light κ	$0.1346, 0.1351, 0.1353$	$0.13344, 0.13417, 0.13455$
κ_{crit}	0.13581^{+2}_{-1}	0.13525^{+2}_{-1}
κ_{n}	0.13578^{+1}_{-2}	0.13520^{+1}_{-2}
κ_{s}	0.13495^{+2}_{-1}	0.13476^{+3}_{-5}

re-samplings. Unless otherwise specified, all errors listed in tables are statistical. The lattice spacing has been fixed by using the force scale r_0 [11,12].

2.4 Improvement Coefficients

The improvement programme requires values for the current and mass improvement and renormalisation coefficients defined in equations (2), (3) and (6) in Section 2.1. One would like to use non-perturbative determinations of the coefficients in order to remove all $\mathcal{O}(a)$ errors. Where this is not possible perturbation theory must be used, although this leaves residual discretisation errors of $\mathcal{O}(\alpha_{\mathrm{s}} a)$.

Non-perturbative values for Z_{A}, Z_{V}, c_{A}, b_{A} and b_{V} are used. There is no reliable non-perturbative value for the vector current improvement coefficient, c_{V}. The ALPHA collaboration's preliminary NP determination [13,14] is an order of magnitude larger than the perturbative value and has a large uncertainty. The determination by Bhattacharya *et al.* [15,16] has a very large uncertainty. Therefore, the perturbative coefficient [17] is employed. The perturbative value of the mass improvement coefficient, b_{m}, is used [2] . The improvement coefficients appear, with references, in Table 2. Perturbative determinations are denoted by BPT in the table and are evaluated using a boosted coupling $g^2 = g_0^2/u_0^4$. The mean link, u_0, is taken from the plaquette expectation value,

---

[2] A non-perturbative determination of b_{m} exists at $\beta = 6.2$ [18]. The BPT value agrees at one standard deviation. The choice of value used makes little difference to the final results.

Table 2
Improvement coefficients used in this work. Authors' quoted errors have been combined in quadrature.

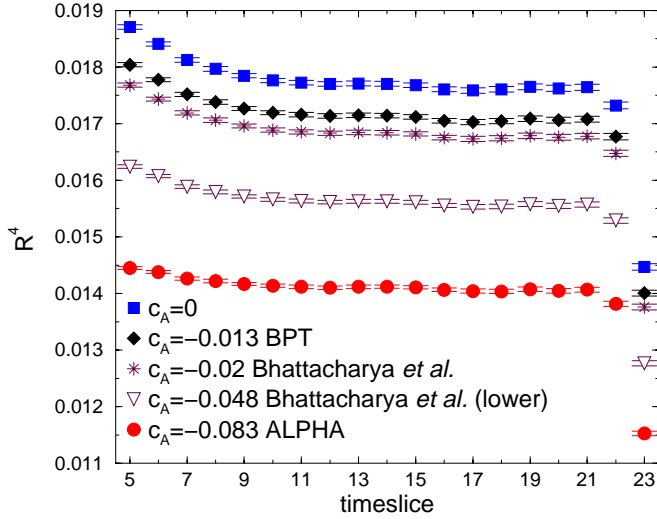| Coefficient	Ref.	$\beta = 6.2$	$\beta = 6.0$
c_A	NP [5]	-0.0371	-0.0828
c_V	BPT [17]	-0.0258	-0.0275
Z_A	NP [19]	$0.8067(79)$	$0.7906(94)$
Z_V	NP [19]	$0.7922(10)$	$0.7809(6)$
b_A	NP [15,16]	$1.47(12)$	$1.44(13)$
b_V	NP [19]	$1.404(7)$	$1.477(7)$
b_m	BPT [17]	-0.652	-0.662

Fig. 1. The mixing of the axial current with the pseudoscalar density. $\beta = 6.0$, $\kappa_H = 0.1123$, $\kappa_L = 0.13344$. The ratio plotted is defined in equation (13).

$u_0^4 = \langle \mathrm{Re}\,\mathrm{Tr}\,U_\mathrm{P} \rangle / 3$.

Changes in c_A and c_V can have a particularly large effect on the extracted values of the decay constants when the pseudoscalar and vector meson masses are not small (in lattice units), since the improved current matrix elements are given by,

$$\langle 0|A_4^\mathrm{I}|P\rangle = \langle 0|A_4|P\rangle + c_A \sinh(aM_P)\langle 0|P|P\rangle \qquad (9)$$
$$\langle 0|V_i^\mathrm{I}|V,\epsilon\rangle = \langle 0|V_i|V,\epsilon\rangle + c_V \sinh(aM_V)\langle 0|T_{i4}|V,\epsilon\rangle$$

when the ground state is isolated. In particular at $\beta = 6.0$ the heavy-light meson mass at the heaviest kappa is bigger than one and thus $\sinh aM \sim 1.3$.
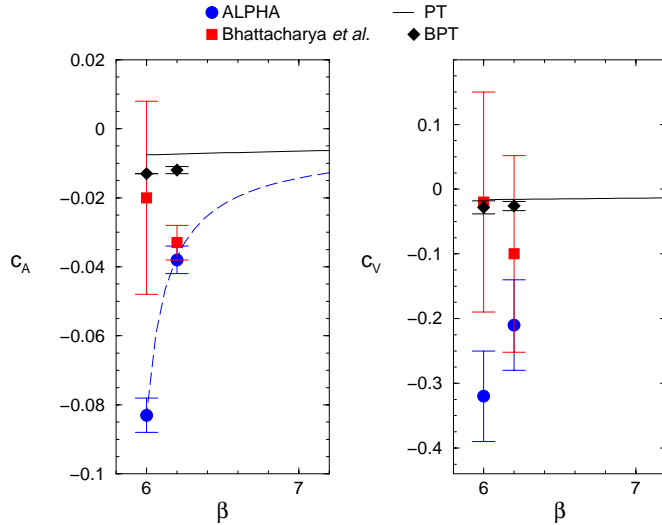
Fig. 2. The improvement coefficients c_A (left) and c_V (right) as functions of the coupling β. Note that the vertical scales in the two plots are different. The values of the coefficients are shown for the two values of the coupling used in this work. The dashed line through the ALPHA c_A points is their interpolating function.

This is illustrated for the pseudoscalar decay constant in Figure 1. The figure shows the ratio R^4 (defined in equation (13) below), which is proportional to f_P, for several different values of c_A at $\beta = 6.0$. It can be seen that using the NP value of c_A from the ALPHA collaboration [5] decreases R^4 by $\sim 20\%$ compared to $c_A = 0$. The plot also shows the ratio determined using the NP value of c_A from Bhattacharya et al. [15,16] and its lower error bar (denoted "lower" in the plot legend), illustrating that an imprecisely determined improvement coefficient would result in a large uncertainty in the decay constant.

In Tables 4 and 5 the last column shows the effect on the vector meson decay constant of using the preliminary NP determination of c_V [13,14]. For $\beta = 6.0$, $c_V^{NP} = -0.32 \pm 0.06$, and for the heaviest mass, $c_V \sinh aM_V = -0.48$. This makes the vector decay constant 60% bigger than with c_V^{BPT}.

Clearly, reliable determinations of the improvement coefficients are highly desirable. The various determinations of both c_A and c_V are shown in Figure 2. The different determinations of the coefficients are not considered as systematic uncertainties in this calculation of the decay constants because, at least at $\beta = 6.0$, some of the determinations are inconsistent at the level of several sigma. Thus, the best current values for these coefficients are chosen, and fluctuations between the different determinations are not included in the systematic uncertainties in this work. However, should future determinations yield substantially different values for the coefficients, the results in this work would change significantly.

Table 3
Pseudoscalar and vector masses in lattice units at $\beta = 6.2$ and $\beta = 6.0$. Fit ranges
are $12 - 22$ at $\beta = 6.2$ and $10 - 22$ (P), $10 - 21$ (V) at $\beta = 6.0$.

	$\beta = 6.2$				$\beta = 6.0$		
κ_H	κ_L	aM_P	aM_V	κ_H	κ_L	aM_P	aM_V
	0.1346	0.841^{+1}_{-1}	0.871^{+2}_{-2}		0.13344	1.145^{+2}_{-1}	1.188^{+2}_{-2}
0.1200	0.1351	0.823^{+2}_{-1}	0.856^{+2}_{-2}	0.1123	0.13417	1.121^{+2}_{-2}	1.166^{+3}_{-3}
	0.1353	0.817^{+2}_{-1}	0.848^{+3}_{-2}		0.13455	1.110^{+3}_{-2}	1.158^{+4}_{-4}
	0.1346	0.739^{+1}_{-1}	0.775^{+2}_{-2}		0.13344	1.006^{+2}_{-1}	1.056^{+2}_{-2}
0.1233	0.1351	0.721^{+2}_{-1}	0.759^{+2}_{-2}	0.1173	0.13417	0.981^{+2}_{-2}	1.034^{+3}_{-2}
	0.1353	0.714^{+2}_{-1}	0.752^{+3}_{-2}		0.13455	0.969^{+2}_{-2}	1.026^{+4}_{-4}
	0.1346	0.628^{+1}_{-1}	0.673^{+2}_{-2}		0.13344	0.851^{+1}_{-1}	0.915^{+2}_{-2}
0.1266	0.1351	0.609^{+1}_{-1}	0.656^{+2}_{-2}	0.1223	0.13417	0.825^{+2}_{-1}	0.892^{+3}_{-2}
	0.1353	0.602^{+2}_{-1}	0.650^{+3}_{-2}		0.13455	0.811^{+2}_{-2}	0.883^{+4}_{-3}
	0.1346	0.505^{+1}_{-1}	0.563^{+2}_{-2}		0.13344	0.675^{+1}_{-1}	0.759^{+2}_{-2}
0.1299	0.1351	0.484^{+1}_{-1}	0.546^{+2}_{-2}	0.1273	0.13417	0.646^{+2}_{-1}	0.736^{+3}_{-2}
	0.1353	0.476^{+1}_{-1}	0.540^{+2}_{-2}		0.13455	0.631^{+2}_{-1}	0.727^{+4}_{-3}

2.5 Extraction of Masses and Decay Constants

The pseudoscalar meson masses are extracted from the asymptotic behaviour
of the two-point correlation functions,

$$
\begin{aligned}
C^{SS}_{PP}(t, \vec{p}) &= \sum_{\vec{x}} e^{-i\vec{p}\cdot\vec{x}} \langle \Omega^S_P(t, \vec{x})\Omega^{S\dagger}_P(0, \vec{0})\rangle \\
&\stackrel{t\to\infty}{\to} \frac{\left(Z^S_P(\vec{p})\right)^2}{2aE_P} \cosh(aE_P(t - T/2))e^{-aE_P T/2}
\end{aligned}
\tag{10}
$$

where $T = 48$ and aE_P is the energy of the lowest lying meson destroyed by the
operator Ω^S_P and created by $\Omega^{S\dagger}_P$. The superscript S denotes a smeared, or spa-
tially extended, interpolating field operator constructed using the technique
described in [20]. $Z^S_P(\vec{p})$ is the overlap of the operator with the pseudoscalar
state given by $Z^S_P(\vec{p}) = \langle 0|\Omega^S_P(0, \vec{0})|\mathrm{P}(\vec{p})\rangle$.

A similar procedure is used to extract the masses of vector mesons from corre-
lation functions constructed with the appropriate vector operators. Fit ranges
are established by inspection of the time-dependent effective mass. The masses
are shown in Table 3.

The decay constants are extracted from the asymptotic behaviour of different two-point correlation functions. The momentum dependence of the matrix elements and energies are suppressed from now on, as the decay constants are all extracted at zero momentum. For the pseudoscalar decay constant, the PA correlation function at large times is used:

$$
\begin{aligned}
C_{PA}^{SL}(t, \vec{0}) &= \sum_{\vec{x}} \langle A_4^{\mathrm{I}}(t, \vec{x}) \Omega_P^{S\dagger}(0, \vec{0}) \rangle \\
&\stackrel{t \to \infty}{\to} \frac{Z_A^L Z_P^S}{2aM_P} \sinh(aM_P(t - T/2)) e^{-aM_P T/2}
\end{aligned}
\tag{11}
$$

where A_4^{I} is the time component of the improved axial current operator defined in equation (2). The superscript L on the correlator denotes a local operator, in this case the axial current. $Z_A^L = \langle 0|A_4^{\mathrm{I}}|P(\vec{0})\rangle$ is the overlap of the local axial operator with the pseudoscalar state, from which the decay constant can be extracted using equations (3) and (7).

Extraction of the vector decay constant involves the large time behaviour of the VV correlation function:

$$
\begin{aligned}
C_{VV}^{SL}(t, \vec{0}) &= \sum_j \sum_{\vec{x}} \langle V_j^{\mathrm{I}}(t, \vec{x}) \Omega_{V_j}^{S\dagger}(0, \vec{0}) \rangle \\
&\stackrel{t \to \infty}{\to} \frac{Z_V^L Z_V^S}{2aM_V} \cosh(aM_V(t - T/2)) e^{-aM_V T/2}
\end{aligned}
\tag{12}
$$

where V_j^{I} is a spatial component of the improved local vector current operator. Again, S denotes a smeared or spatially extended interpolating field operator and L a local operator. The factor Z_V^L is the overlap of the local vector operator with the vector state, $Z_V^L = \sum_r \epsilon_k^r \langle 0|V_k^{\mathrm{I}}|V(\vec{0}, \vec{\epsilon})\rangle$, from which the vector decay constant can be extracted via equation (8).

Matrix elements proportional to the decay constants are extracted from ratios of correlation functions with different smearing combinations. The pseudoscalar decay constant is extracted from the ratio of the axial to the pseudoscalar correlation function,

$$
R^4 \equiv \frac{C_{PA}^{SL}(t)}{C_{PP}^{SS}(t)} \stackrel{t \to \infty}{\to} \frac{Z_A^L}{Z_P^S} \tanh(aM_P(T/2 - t))
\tag{13}
$$

This ratio is shown in Figure 1 for various values of c_{A}. The vector decay constant is determined from the ratio,

$$
\frac{C_{VV}^{SL}(t)}{C_{VV}^{SS}(t)} \stackrel{t \to \infty}{\to} \frac{Z_V^L}{Z_V^S}
\tag{14}
$$

Table 4
Pseudoscalar and vector decay constants in lattice units at $\beta = 6.2$. Fit ranges are
$14 - 21$ (P) and $15 - 23$ (V).

κ_{H}	κ_{L}	af_P	$f_V(c_{\mathrm{V}}\mathrm{BPT})$	$f_V(c_{\mathrm{V}}\mathrm{NP})$
	0.1346	0.0889^{+8}_{-8}	8.53^{+9}_{-9}	10.2^{+1}_{-1}
0.1200	0.1351	0.0844^{+8}_{-9}	8.8^{+1}_{-1}	10.4^{+1}_{-1}
	0.1353	0.0828^{+9}_{-9}	8.9^{+1}_{-1}	10.5^{+2}_{-1}
	0.1346	0.0867^{+7}_{-7}	7.61^{+7}_{-7}	8.81^{+9}_{-8}
0.1233	0.1351	0.0823^{+7}_{-8}	7.79^{+9}_{-9}	9.0^{+1}_{-1}
	0.1353	0.0808^{+8}_{-9}	7.9^{+1}_{-1}	9.0^{+1}_{-1}
	0.1346	0.0839^{+6}_{-7}	6.62^{+6}_{-6}	7.46^{+7}_{-7}
0.1266	0.1351	0.0797^{+7}_{-8}	6.73^{+7}_{-7}	7.56^{+8}_{-8}
	0.1353	0.0782^{+7}_{-9}	6.76^{+9}_{-7}	7.6^{+1}_{-1}
	0.1346	0.0792^{+6}_{-7}	5.57^{+5}_{-5}	6.11^{+6}_{-5}
0.1299	0.1351	0.0754^{+6}_{-8}	5.60^{+6}_{-5}	6.12^{+6}_{-5}
	0.1353	0.0740^{+6}_{-9}	5.61^{+7}_{-5}	6.12^{+7}_{-6}

An alternative method is simultaneously to fit several correlators to estimate
the contamination of the ground state signal coming from excited states. In
this case an eight parameter simultaneous fit to three different correlators,
C_{PP}^{SS}, C_{PA}^{SL} and C_{PP}^{SL}, is used, allowing for ground and first excited state con-
tributions. This gives consistent answers for the pseudoscalar decay constant.
The ratio method is used for central values in the following, but the difference
from the multi-exponential fits is quoted below as one measure of systematic
error (see Table 10). Results for the decay constants are shown in Tables 4
and 5.

3 Extrapolation in the Quark Masses

With the ultraviolet cutoffs currently available, and using the SW fermion
action, only mesons with masses up to about 2.4 GeV can be studied directly
with acceptably small lattice artefacts. Moreover, input light quark masses are
above $m_{\mathrm{s}}/2$ owing to critical slowing down of quark propagator calculations,
and potential finite volume effects. Extrapolation or interpolation in quark
masses must be performed to extract physical masses and decay constants.

Table 5

Pseudoscalar and vector decay constants in lattice units at $\beta = 6.0$. Fit ranges are $14 - 21$ (P) and $16 - 23$ (V).

κ_{H}	κ_{L}	af_P	$f_V(c_{\mathrm{V}}\mathrm{BPT})$	$f_V(c_{\mathrm{V}}\mathrm{NP})$
	0.13344	0.111^{+1}_{-1}	7.9^{+1}_{-1}	12.7^{+2}_{-1}
0.1123	0.13417	0.106^{+1}_{-1}	8.0^{+1}_{-1}	12.7^{+2}_{-2}
	0.13455	0.104^{+1}_{-1}	8.0^{+2}_{-1}	12.5^{+3}_{-2}
	0.13344	0.1091^{+8}_{-9}	7.11^{+8}_{-7}	10.3^{+1}_{-1}
0.1173	0.13417	0.104^{+1}_{-1}	7.2^{+1}_{-1}	10.3^{+1}_{-1}
	0.13455	0.103^{+1}_{-1}	7.2^{+1}_{-1}	10.2^{+2}_{-2}
	0.13344	0.1056^{+7}_{-8}	6.26^{+7}_{-6}	8.34^{+9}_{-8}
0.1223	0.13417	0.1010^{+8}_{-9}	6.31^{+8}_{-8}	8.3^{+1}_{-1}
	0.13455	0.099^{+1}_{-1}	6.3^{+1}_{-1}	8.2^{+1}_{-1}
	0.13344	0.1000^{+6}_{-8}	5.30^{+6}_{-5}	6.54^{+7}_{-7}
0.1273	0.13417	0.0956^{+6}_{-9}	5.29^{+7}_{-6}	6.45^{+8}_{-8}
	0.13455	0.094^{+1}_{-1}	5.22^{+8}_{-7}	6.3^{+1}_{-1}

3.1 Chiral Extrapolations

The light, or normal, quark mass m_{n}, defined by $m_{\mathrm{n}} \equiv (m_{\mathrm{u}} + m_{\mathrm{d}})/2$, and strange quark mass m_{s} are determined from the light hadron spectrum using the lowest order chiral perturbation theory relation for the mass of a pseudoscalar meson with quark content q_1 and q_2,

$$(am_{\mathrm{P}})^2 = B(a\widetilde{m}_{q_1} + a\widetilde{m}_{q_2}) \tag{15}$$

where the rescaled quark mass $\widetilde{m}_{\mathrm{q}}$ is defined in equation (6). The corresponding hopping parameters, together with κ_{crit}, corresponding to zero quark mass, are taken from a previous UKQCD calculation [9] and listed in Table 1.

A linear dependence of heavy-light masses and decay constants on the light quark mass is assumed:

$$aK_i = \alpha_i + \beta_i a\widetilde{m}_{\mathrm{q}} \tag{16}$$

where K_i is f_P, f_V/a, m_{P} or m_{V}. Some example extrapolations are shown in Figure 3. The results for the extrapolated quantities are shown in Tables 6 and 7.
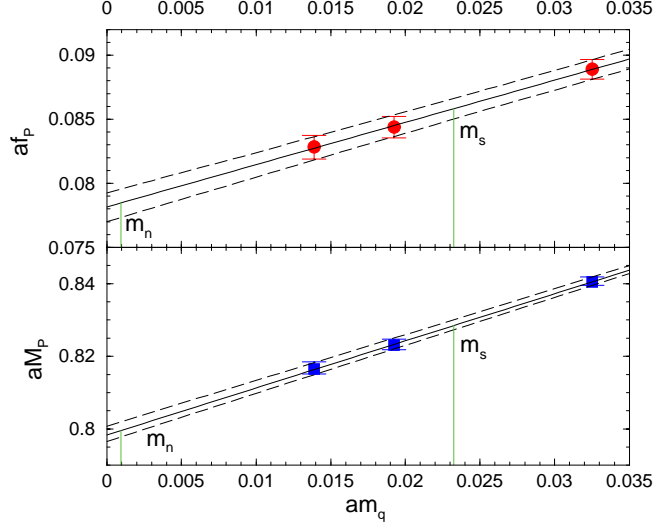
Fig. 3. The chiral extrapolation of the pseudoscalar decay constant (top) and pseudoscalar mass (bottom) against rescaled light quark mass. $\beta = 6.2$ and $\kappa_H = 0.1200$. The vertical lines show the strange and normal quark masses.

Table 6
Masses and decay constants at physical light quark masses. $\beta = 6.2$.

κ_H	κ_L	aM_P	af_P	aM_V	f_V
0.1200	κ_n	0.800(2)	0.078(1)	0.832(4)	9.0(1)
	κ_s	0.828(2)	0.0858(8)	0.860(2)	8.6(1)
0.1233	κ_n	0.696(2)	0.077(1)	0.736(3)	8.0(1)
	κ_s	0.726(1)	0.0837(8)	0.764(2)	7.68(9)
0.1266	κ_n	0.583(2)	0.074(1)	0.634(3)	6.8(1)
	κ_s	0.615(1)	0.0810(8)	0.661(2)	6.66(7)
0.1299	κ_n	0.455(2)	0.070(1)	0.523(3)	5.6(1)
	κ_s	0.491(1)	0.0766(8)	0.551(1)	5.57(6)

3.2 Heavy Quark Extrapolations

Heavy Quark Symmetry (HQS) implies asymptotic scaling laws [21] for the decay constants in the infinite heavy quark mass limit. Away from this limit, heavy quark effective theory ideas motivate the following ansätze for the dependence on the heavy meson masses:

$$\Phi_{\mathrm{P}}(M_P) \equiv \Theta(M_{\mathrm{B}}, M_P) f_P \sqrt{M}_P = \gamma_{\mathrm{P}}(1 + \frac{\delta_{\mathrm{P}}}{M_P} + \frac{\eta_{\mathrm{P}}}{M_P^2}) \tag{17}$$

12

Table 7
Masses and decay constants at physical light quark masses. $\beta = 6.0$.

κ_H	κ_L	aM_P	af_P	aM_V	f_V
	κ_n	1.087(4)	0.099(2)	1.138(5)	8.0(2)
0.1123	κ_s	1.125(2)	0.106(1)	1.171(3)	7.9(1)
	κ_n	0.945(3)	0.098(1)	1.005(5)	7.2(2)
0.1173	κ_s	0.985(2)	0.105(1)	1.039(3)	7.1(1)
	κ_n	0.786(3)	0.095(1)	0.862(5)	6.3(1)
0.1223	κ_s	0.829(2)	0.1019(9)	0.897(3)	6.22(8)
	κ_n	0.603(2)	0.090(1)	0.704(5)	5.2(1)
0.1273	κ_s	0.651(2)	0.0965(8)	0.740(3)	5.23(7)

$$\Phi_{\mathrm{V}}(M_V) \equiv \Theta(M_{\mathrm{B}}, M_V)\frac{M_V}{f_V}\sqrt{M_V} = \gamma_{\mathrm{V}}(1 + \frac{\delta_{\mathrm{V}}}{M_V} + \frac{\eta_{\mathrm{V}}}{M_V^2}) \tag{18}$$

where Θ denotes logarithmic corrections given at leading order by [22],

$$\Theta(M_{\mathrm{B}}, M) = \left(\frac{\alpha(M)}{\alpha(M_{\mathrm{B}})}\right)^{2/\beta_0} \tag{19}$$

Here, β_0 is the one-loop QCD beta function coefficient, equal to 11 in the quenched approximation, and $\Lambda_{\overline{\mathrm{MS}}}^{(4)} = 295$ MeV [23]. The extrapolation in the heavy meson mass for the pseudoscalar decay constant at $\beta = 6.2$ is shown in Figure 4.

HQS also relates the pseudoscalar and vector decay constants as follows [22];

$$U(\overline{M}) \equiv \frac{f_V f_P}{\overline{M}} = \left(1 + \frac{8}{3}\frac{\alpha_s(\overline{M})}{4\pi} + \mathcal{O}(1/\overline{M})\right) \tag{20}$$

where $\overline{M} \equiv (M_P + 3M_V)/4$ is the spin-averaged heavy meson mass. The one-loop factor Θ in equations (17) and (18) cancels in the ratio in equation (20). Higher order QCD corrections produce the term proportional to α_{s}. $\tilde{U}(\overline{M})$ is defined to eliminate the radiative corrections in $U(\overline{M})$

$$\tilde{U}(\overline{M}) \equiv U(\overline{M}) / \left\{1 + \frac{8}{3}\frac{\alpha_{\mathrm{s}}(\overline{M})}{4\pi}\right\} \tag{21}$$

Calculated values of $\widetilde{U}(\overline{M})$ are fitted to the following parameterisation:

$$\widetilde{U}(\overline{M}) = \omega_0 + \frac{\omega_1}{\overline{M}} + \frac{\omega_2}{\overline{M}^2} \qquad (22)$$

HQS implies that $\omega_0 = 1$. However, ω_0 can also be left as a free parameter to test the applicability of HQS. Likewise, HQS can be applied to set $\gamma_P = \gamma_V$ in fits using equations (17) and (18). However, higher order QCD corrections would modify this in a similar way to $\widetilde{U}(\overline{M})$, that is

$$\frac{\gamma_P}{\gamma_V} = \left(1 + \frac{8}{3}\frac{\alpha_s(\overline{M})}{4\pi}\right) \qquad (23)$$

Two alternative procedures are tried to estimate the systematic error in determining the decay constants at the b quark mass arising from this extrapolation. First a linear fit, that is dropping the η term from equations (17) and (18), is made to the decay constants with the heaviest three quark masses. Second, a quadratic fit is made to the decay constants at all values of heavy quark mass, imposing the HQS constraint described above. For the extrapolation to the b quark mass, the variation in the two methods is smaller than that coming from different definitions of the lattice spacing. Obtaining the decay constants at the charm quark mass requires only an interpolation, consequently the systematic error for charm decay constants is small.

4   Decay Constants

Results for the decay constants at physical meson masses are shown in Table 8. The extrapolation in the heavy meson mass for the pseudoscalar decay constant at $\beta = 6.2$ is shown in Figure 4. The difference between a quadratic fit to all four points and a linear fit to the heaviest three can be seen. This has no effect for the D meson, but is one of the main uncertainties in the B meson decay constant. The dot-dashed and dashed lines show the meson masses (B and D) with the scale set by r_0, and m_ρ respectively. Once the explicit scale dependence of $\Phi_P(M_P)$ is considered, the scale-setting is responsible for the largest systematic uncertainty in this calculation (*cf.* Table 10).

Lattice QCD determinations of the pseudoscalar meson decay constants generally find $f_D > f_B$ [24,25]. In this work, setting the scale from r_0 and using a quadratic fit in the heavy mass extrapolation results in $f_D \sim f_B$, as quoted in the Introduction. However, as Table 8 reveals, other choices of scale-setting and extrapolation procedure (quadratic or linear), do lead to $f_D > f_B$ and give generally lower values overall.
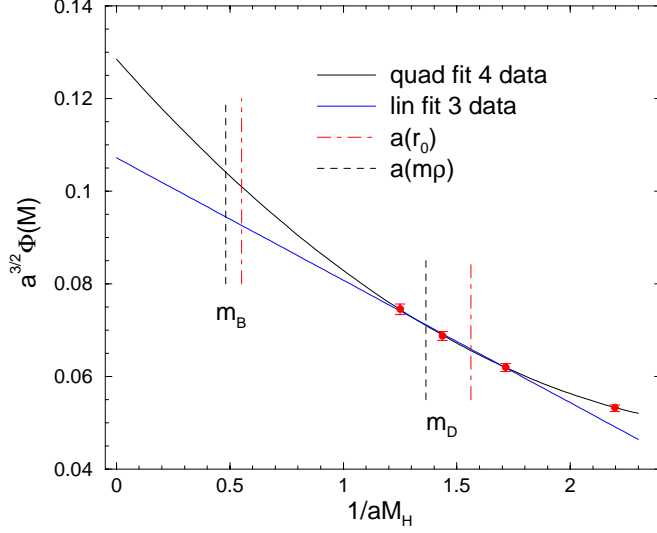
14

Fig. 4. The extrapolation of the pseudoscalar decay constant in heavy meson mass at $\beta = 6.2$.

Table 8
The decay constants at both β values with the scale set by r_0 or m_ρ and a quadratic (Q) or linear (L) fit for the extrapolation in inverse heavy meson mass. The quadratic fit uses all four heavy masses, while the linear fit uses the heaviest three.

		$\beta = 6.2$				$\beta = 6.0$			
		f_P(MeV)		f_V		f_P(MeV)		f_V	
		Q	L	Q	L	Q	L	Q	L
	B	218(5)	200(4)	22.6(7)	23.8(7)	196(6)	183(4)	18.9(8)	20.4(8)
	D	220(3)	221(3)	7.5(1)	7.4(1)	206(3)	207(3)	6.7(2)	6.8(2)
r_0	B_s	242(4)	222(3)	20.9(4)	22.0(4)	213(4)	198(3)	18.1(5)	19.5(4)
	D_s	241(2)	242(2)	7.3(1)	7.3(1)	221(2)	222(2)	6.9(1)	6.8(1)
	B	186(4)	169(3)	26.4(8)	28.5(8)	170(5)	158(4)	21(1)	24(1)
	D	197(3)	198(3)	8.5(2)	8.6(2)	187(3)	187(3)	7.5(2)	7.5(1)
m_ρ	B_s	212(3)	193(2)	23.5(4)	25.4(4)	189(3)	175(2)	19.8(5)	22.2(4)
	D_s	221(2)	222(2)	8.1(1)	8.1(1)	204(2)	204(2)	7.5(1)	7.4(1)

The applicability of HQS in the range of quark masses used in this work can be examined by comparing the decay constants extracted with or without the HQS constraint equation (23). This is shown in Figure 5 for both values of β. At $\beta = 6.2$ the constraint makes no significant difference whilst at $\beta = 6.0$ the difference is quite large. A natural explanation is that higher order discretisation effects are spoiling the scaling behaviour, since the range of masses is similar for both values of β. It is clear from the figure that the
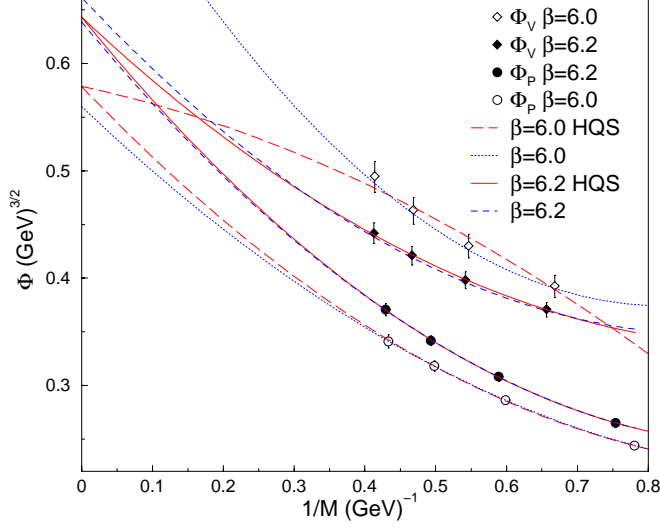
Fig. 5. The extrapolation of the decay constants to the infinite quark mass limit, with and without the HQS constraint. The solid (long dashed) lines show the extrapolation with the constraint at $\beta = 6.2$ ($\beta = 6.0$). The dashed (dotted) lines show the extrapolation without the constraint at $\beta = 6.2$ ($\beta = 6.0$).
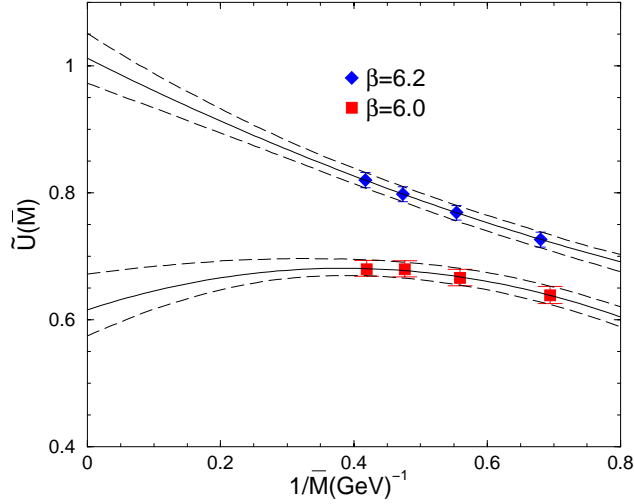

Fig. 6. The quantity $\widetilde{U}(\overline{M})$ as a function of the inverse spin averaged mass $\overline{M}$.

Table 9
$\widetilde{U}(\overline{M})$ as a function of heavy meson mass.

β	$\overline{M}_{\mathrm{D}}$	$\overline{M}_{\mathrm{B}}$	$\overline{M}_{\infty}$
6.2	0.79(1)	0.92(2)	1.01(4)
6.0	0.67(1)	0.66(3)	0.62(6)

pseudoscalar and vector Φ functions have a different trend in β. The quantity $\widetilde{U}(\overline{M})$ in equation (20) which parameterises the deviation from the heavy quark limit is shown in Figure 6 and Table 9, further illustrating this point.
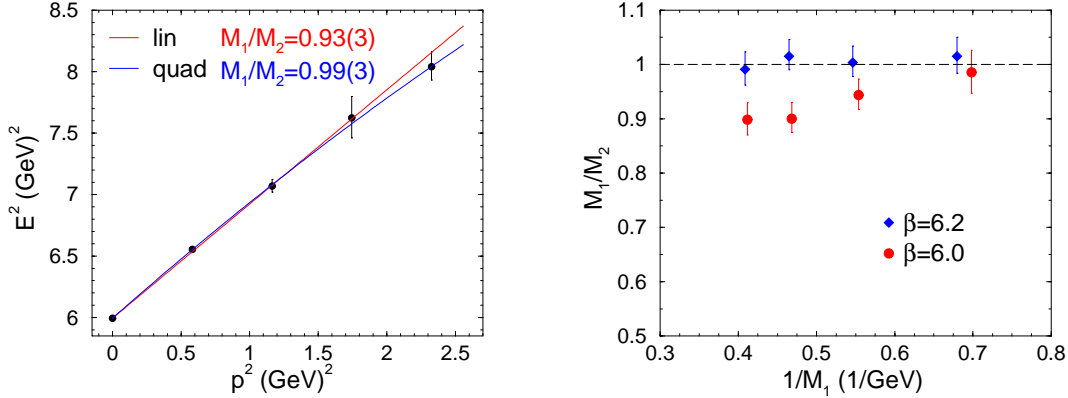
16

Fig. 7. Left: the pseudoscalar dispersion relation for $\kappa_H = 0.1200$, $\kappa_L = 0.1346$ in physical units at $\beta = 6.2$. Right: the ratio M_1/M_2 as a function of M_1.

Whilst the theory employed is $\mathcal{O}(a)$ improved, $\mathcal{O}(a^2)$ effects may still be important at any fixed lattice spacing. In particular, $\mathcal{O}(a^2 m^2)$ effects could well be significant for heavy quarks. One of the effects of discretising space-time is to alter the free particle dispersion relation. The lattice dispersion relation can be written

$$E^2 = M_1^2 + \frac{M_1}{M_2}\vec{p}^{\,2} + \mathcal{O}(p^4) \tag{24}$$

where M_1 is the energy at zero momentum and M_2 is the kinetic mass, defined by $M_2^{-1} = \partial^2 E/\partial p_i^2|_{\vec{p}=0}$. The dispersion relation is investigated by fitting hadronic correlators computed at five different momentum values ($\vec{p}^{\,2} = 0, 1, 2, 3, 4$ in lattice units) using linear and quadratic fits in $\vec{p}^{\,2}$. The fit for the heaviest quark combination at $\beta = 6.2$ is shown on the left of Figure 7. A quadratic fit to the data gives an estimate of M_1/M_2 close to unity. The data is linear up to $\vec{p}^{\,2} = 1.5$ GeV, *i.e.* in good agreement with the continuum dispersion relation. The right hand side of Figure 7 shows the M_1/M_2 estimates for all available heavy quarks. At $\beta = 6.2$ all values are consistent with unity suggesting that discretisation errors are small. At $\beta = 6.0$, M_1/M_2 deviates systematically from unity reflecting the onset of discretisation effects with larger lattice spacing.

It is possible to estimate higher order discretisation effects with the KLM normalisation [26]. In this prescription, based on the comparison between a free lattice quark propagator and its continuum equivalent, the normalisation of the quark fields is changed as follows,

$$\psi \rightarrow \psi' = \sqrt{1 + am}\,\psi \tag{25}$$

in order to eliminate $\mathcal{O}((am)^n)$ effects to all orders. However, in the $\mathcal{O}(a)$ improved theory the $\mathcal{O}(am)$ errors are already accounted for. This suggests

17

the following KLM-like modification (as used in [27]) to the normalisation of the heavy-light current

$$Z_{\mathrm{A}}(1 + b_{\mathrm{A}}am_{\mathrm{eff}}) \rightarrow Z_{\mathrm{A}}(1 + b_{\mathrm{A}}am_{\mathrm{eff}})\frac{\sqrt{1 + am_Q}\sqrt{1 + am_q}}{1 + am_{\mathrm{eff}}} \qquad (26)$$

where $am_{\mathrm{eff}} = am_Q/2 + am_q/2$. At $\beta = 6.2$, the quark masses, in lattice units, are all less than one half. Consequently the factor in equation (26) is near unity. The decay constants at the D and B meson scales are negligibly different with and without the KLM factor. At $\beta = 6.0$ the quark masses, in lattice units, are larger than at $\beta = 6.2$ and so the KLM factor is larger. The values of f_{D} and f_{B} are lower by 2% and 8% respectively. This corroborates evidence from the HQS scaling of the decay constants and the value of b_{m} from the heavy-light spectrum (see section 5), that higher order discretisation effects are significant at $\beta = 6.0$, but much smaller at $\beta = 6.2$.

The improvement coefficient c_{A} is precisely determined by the ALPHA collaboration. The coefficient b_{A} listed in Table 2, however, has a larger error, which has a noticeable effect on the value of the pseudoscalar decay constants. This is quantified in Table 10 which shows the variation induced using the extreme values of b_{A} compared to the central value.

The continuum limit can be investigated by comparing results at different β values. In this calculation, the uncertainty in the decay constants at a given β originating from the method used to set the scale is larger than the difference between β values using the same method to set the scale. This is shown in Figure 8. Central values are quoted from results at $\beta = 6.2$ with the difference between the results at the two β values used to estimate discretisation errors.

The overall systematic error is estimated from varying the procedure used to extract the decay constants. The percentage variations are shown in Table 10. The various errors are then combined in quadrature. No attempt is made to estimate a systematic error arising from different determinations of improvement coefficients, apart from that due to the uncertainty in the NP determination of b_{A} by Bhattacharya et al. [15,16] which is included in estimates of the systematic error of the relevant quantities. The calculation reported here uses the quenched approximation. No systematic error from this source is estimated, or quoted in the results, but the reader may note that initial calculations [28,29] in lattice QCD with two flavours of dynamical quark suggest that heavy-light pseudoscalar decay constants could be larger by as much as 15% in full QCD.

Using the same prescription as Becirevic et al. [27], that is, b_{A} evaluated from BPT and the scale set by their value of m_{K^*} ($a^{-1} = 2.75$ GeV) with a linear heavy extrapolation using the KLM normalisation, gives values for f_{B}

Table 10

Percentage systematic uncertainties. Systematic differences are obtained by varying the procedure to calculate the decay constants, where the following are used to fix the central values: using r_0 to set the scale at $\beta = 6.2$, a quadratic heavy quark extrapolation, the central value of b_A, fitting correlation functions to a single exponential, using m_K^2 to set the strange quark mass.

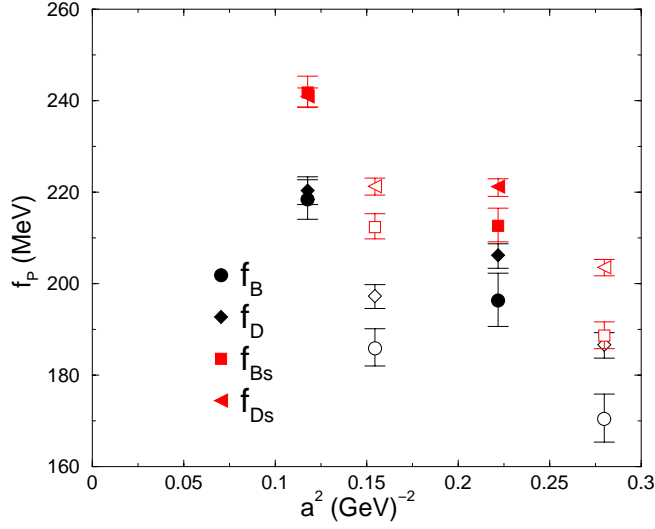| Pseudoscalar	f_B	f_D	f_{B_s}	f_{D_s}	$\frac{f_{B_s}}{f_B}$	$\frac{f_{D_s}}{f_D}$
scale set by m_ρ	15	10	12	8	3	3
$\beta = 6.0$	10	6	12	8	2	2
heavy meson extrapolation	8	–	8	–	–	–
coeff. b_A	5	2	5	2	–	–
multi-exp	6	4	4	3	3	2
strange quark mass	–	–	2	2	2	2
Vector	f_{B^*}	f_{D^*}	$f_{B_s^*}$	$f_{D_s^*}$	$\frac{f_{B_s^*}}{f_{B^*}}$	$\frac{f_{D_s^*}}{f_{D^*}}$
scale set by m_ρ	18	17	14	12	3	3
$\beta = 6.0$	17	9	14	6	4	2
heavy meson extrapolation	7	–	7	–	–	–
strange quark mass	–	–	3	1	2	2

Fig. 8. The dependence of the pseudoscalar decay constants on the method of setting the scale, at two values of β. The closed (open) symbols have the scale set by r_0 (m_ρ).

Table 11
f_B(MeV) at $\beta = 6.2$: comparison with Becirevic *et al.* [27], using the same procedure.

	Becirevic *et al.*	this work
quadratic fit	205 ± 24	184 ± 4
linear fit	179 ± 18	172 ± 3

Table 12
Flavour-breaking ratios.

β	$\frac{f_{B_s}}{f_B}$	$\frac{f_{D_s}}{f_D}$	$\frac{f_{B_s^*}}{f_{B^*}}$	$\frac{f_{D_s^*}}{f_{D^*}}$
6.2	1.11(1)	1.093(6)	0.92(1)	0.98(1)
6.0	1.08(1)	1.072(6)	0.96(2)	1.00(1)

at $\beta = 6.2$ consistent with their results, as shown in Table 11. Preliminary UKQCD results [30,31] were determined by a similar procedure, but without the KLM normalisation and using m_ρ to set the lattice spacing.

Preliminary results of another UKQCD calculation of the decay constants on the same gauge configurations, but with a tadpole improved fermion action, were reported in [32]. At $\beta = 6.2$, the central values for the decay constants, which lie below ours, can be brought in closer agreement by setting the scale with r_0, as is done here, and by tuning c_A and b_A to the one loop, instead of tree level, values. At $\beta = 6.0$, however, these same modifications worsen the agreement.

The flavour breaking ratios are determined and displayed in Table 12. These ratios, and the decay constants themselves are consistent with other lattice determinations [24,25]. The only experimentally measured heavy-light decay constant is $f_{D_s} = 260 \pm 19 \pm 32 \, \text{MeV}$ [33]. This work agrees within errors.

5 Spectroscopic Quantities

To determine the value of the hopping parameter, κ_c, corresponding to the charm quark mass, an interpolation in heavy quark mass is required. The improved quark mass definition in equation (6) also applies to heavy quarks. For sufficiently heavy mesons, the meson mass is essentially linear in the improved quark mass. The corresponding *bare* quark mass dependence is,

$$aM_H(m_Q) = \rho + \lambda a m_Q + \epsilon a^2 m_Q^2 \tag{27}$$

where $\epsilon/\lambda = b_m$. In the NP improved formulation all lattice artefacts of $\mathcal{O}(a)$ have been removed. However, $\mathcal{O}(a^2 m_Q^2)$ effects for the heaviest quarks could
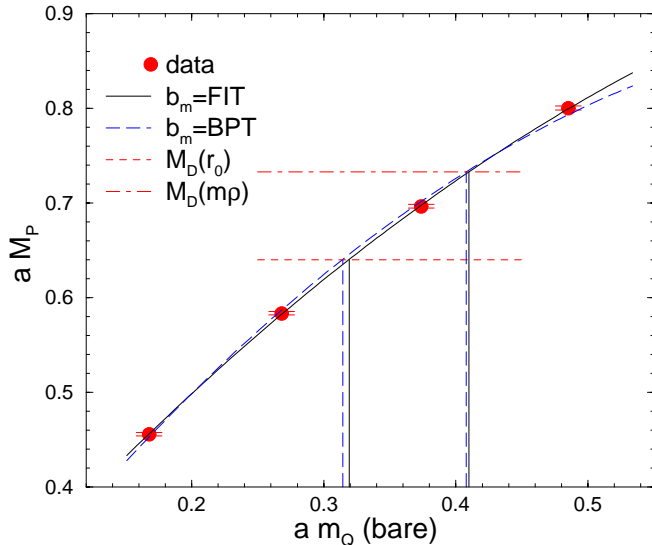
Fig. 9. The pseudoscalar meson vs. bare quark mass for $\beta = 6.2$

Table 13

The hopping parameter corresponding to the charm quark mass. The label FIT refers to the ratio ϵ/λ in equation (27) having a fitted value, whilst BPT refers to the ratio having the BPT value.

| β | $a^{-1}(r_0)$ | | $a^{-1}(m_\rho)$ | |
	FIT	BPT	FIT	BPT
6.2	0.12498^{+6}_{-5}	0.12513^{+6}_{-5}	0.12221^{+7}_{-5}	0.12227^{+7}_{-5}
6.0	0.11952^{+8}_{-6}	0.12056^{+8}_{-6}	0.1160^{+1}_{-1}	0.1165^{+2}_{-2}

be significant. Any contributions at this order would affect the ratio ϵ/λ such that it was no longer equal to $b_{\rm m}$. A fit to equation (27) is tried with ϵ/λ fixed to $b_{\rm m}$ from boosted perturbation theory, and with ϵ/λ allowed to vary freely [3]. The heavy quark dependence can be used to fix $\kappa_{\rm c}$ by choosing a particular state (or splitting) to have its physical value. Choosing the pseudoscalar mass to fix $\kappa_{\rm c}$, the spectrum of heavy-light mesons can then be predicted.

For $\beta = 6.2$, the results of using equation (27) are shown in Figure 9. Whilst the value of $\epsilon/\lambda = -0.505(4)$ (labelled FIT in the figure) differs somewhat from the value of $b_{\rm m} = -0.652$ from BPT, it makes little difference to the value of the $\kappa_{\rm c}$, of order 0.1%. The choice of quantity to set the lattice spacing clearly has a rather large effect. Values for $\kappa_{\rm c}$ are shown in Table 13, using the free fit to set the value of the hopping parameter.

For $\beta = 6.0$, the value of $\epsilon/\lambda = -0.384(3)$ differs significantly from the value of $b_{\rm m} = -0.662$ from BPT. Consequently the fit using the BPT $b_{\rm m}$ has a very

---

[3] This procedure is entirely equivalent to that of Becirevic *et al.* [27].

large χ^2, as the curvature is too great for the data. The difference in κ_c is still small, of order 1%. For $\beta = 6.2$ the heaviest quark has a value of $am_Q = 0.485$ whereas for $\beta = 6.0$ the heaviest quark has $am_Q = 0.775$. Discretisation errors of $\mathcal{O}(a^2m^2)$ could be responsible for modifying the value of the ratio ϵ/λ. The value of κ_c is rather insensitive to the value of ϵ/λ but because the value of am_Q is so large, the improved quark mass changes dramatically. Using the free fit as the preferred method, the value of κ_c is shown in Table 13.

The spectrum of heavy-light charm states is shown in Figure 10 and is tabulated in Table 14. With only two values of β a continuum extrapolation is not attempted. However, a comparison can be made in order to estimate systematic errors. It is clear from the figure that a large systematic error arises from the definition of the lattice spacing. Depending on which quantity is chosen, different mass splittings appear to be closer to their continuum values. The central values for the spectrum are produced by the following procedures: single exponential fits, using r_0 to set the scale, with ϵ/λ a free parameter in equation (27). The values of the masses at $\beta = 6.2$ are taken to be the central values, with the values at $\beta = 6.0$ used as an estimate of systematic error. The remaining estimates of systematic error come from using multiple exponential fits, using m_ρ to set the scale and in the case of states with a strange quark, using m_{K^*} instead of m_K^2 to set the strange quark mass. All these systematic errors are combined in quadrature. The results, with experimental comparisons, are:

$$
\begin{array}{cc}
\text{Lattice, this work} & \text{Experiment [34]} \\[4pt]
M_{\text{D}_\text{s}} = 1.956^{+2}_{-2}\,{}^{+22}_{-4}\,\text{GeV} & M_{\text{D}^+_\text{s}} = 1.9685^{+5}_{-5}\,\text{GeV} \\[4pt]
M_{\text{D}^*} = 2.002^{+7}_{-6}\,{}^{+16}_{-41}\,\text{GeV} & M_{\text{D}^{*0}} = 2.0067^{+5}_{-5}\,\text{GeV} \\[4pt]
M_{\text{D}^*_\text{s}} = 2.082^{+4}_{-5}\,{}^{+22}_{-31}\,\text{GeV} & M_{\text{D}^{*+}_\text{s}} = 2.1124^{+7}_{-7}\,\text{GeV}
\end{array}
\tag{28}
$$

For the lattice results, the first error is statistical and the second systematic. In this calculation the light quark in each meson is a normal quark. Thus the D* is the isospin-averaged vector state, with mass $M_{\text{D}^*} = (M_{\text{D}^{*0}} + M_{\text{D}^{*\pm}})/2$. With somewhat large systematic errors, the largest of which comes from the lattice spacing, the spectrum is in broad agreement with experiment.

It is also of interest to look at the $M_V - M_P$ splitting as a function of the (pseudoscalar) meson mass. This can be extrapolated to the B scale in inverse mass and to the infinite quark mass limit, where the splitting should vanish. Quenched simulations of heavy-light systems typically underestimate this splitting, and so the extrapolated splitting is also underestimated. The splittings at both values of β are given in Table 15 and are plotted for $\beta = 6.2$ in Figure 11. There is little difference between linear and quadratic fits, so only the linear fit is shown. The splittings obtained from the linear fit at $\beta = 6.2$,
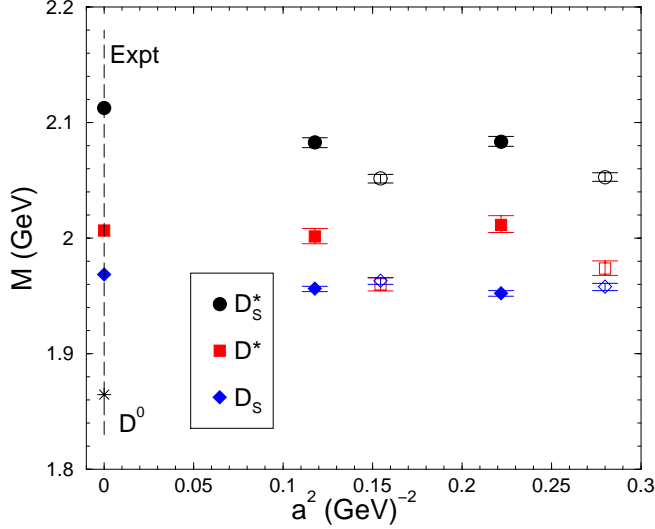
Fig. 10. The scaling of the D meson spectrum. The filled symbols have the lattice spacing set by r_0, and the open symbols by m_ρ.

Table 14
The spectrum of heavy-light mesons with different definitions of the lattice spacing.

	$\beta = 6.2$		$\beta = 6.0$	
state	$a^{-1}(r_0)$	$a^{-1}(m_\rho)$	$a^{-1}(r_0)$	$a^{-1}(m_\rho)$
D_s	1.956^{+2}_{-2}	1.963^{+2}_{-3}	1.952^{+2}_{-2}	1.958^{+3}_{-3}
D^*	2.002^{+7}_{-6}	1.960^{+6}_{-6}	2.011^{+8}_{-7}	1.958^{+3}_{-3}
D_s^*	2.082^{+4}_{-5}	2.052^{+3}_{-4}	2.083^{+4}_{-4}	2.053^{+4}_{-3}

using r_0 to set the scale, are taken as the central values quoted below. The second set of errors is systematic, obtained by combining in quadrature the differences arising from the following variations in procedure (in descending order of importance): using m_ρ rather than r_0 to set the scale; (for the B meson) using a quadratic rather than linear extrapolation; multiple rather than single exponential fits; using $\beta = 6.0$ data rather than $\beta = 6.2$ data. The results, with the comparison to experiment, are as follows:

$$
\begin{array}{cc}
\text{Lattice, this work} & \text{Experiment [34]} \\
M_{D^*} - M_D = 130^{+6+15}_{-6-35} \text{ MeV} & M_{D^*} - M_D = 142.6 \pm 0.5 \text{ MeV} \quad (29) \\
M_{B^*} - M_B = 21^{+7+18}_{-8-16} \text{ MeV} & M_{B^*} - M_B = 45.2 \pm 1.8 \text{ MeV}
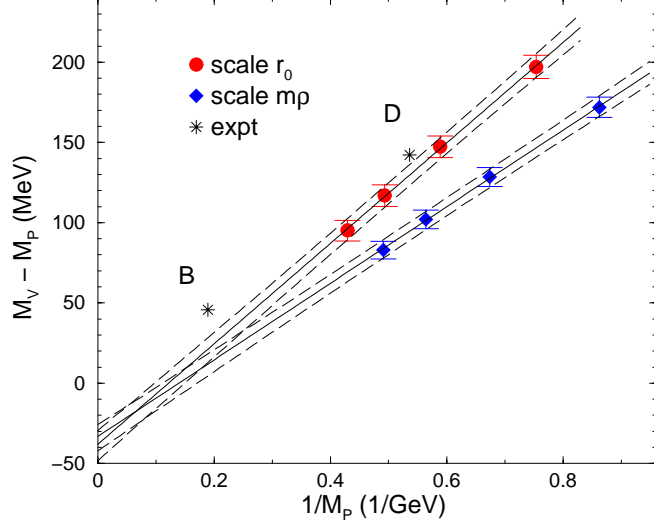\end{array}
$$

Fig. 11. The hyperfine splitting as a function of M in physical units at $\beta = 6.2$. The circles have the scale set by r_0 and the diamonds by m_ρ.

Table 15
The hyperfine splitting of the heavy-light mesons at the B and D meson scale, in MeV

	$\beta = 6.2$		$\beta = 6.0$	
state	$a^{-1}(r_0)$	$a^{-1}(m_\rho)$	$a^{-1}(r_0)$	$a^{-1}(m_\rho)$
$M_{D^*} - M_D$	130^{+7}_{-6}	95^{+6}_{-6}	140^{+8}_{-6}	108^{+7}_{-6}
$M_{B^*} - M_B$	21^{+7}_{-8}	12^{+6}_{-7}	32^{+8}_{-8}	22^{+8}_{-8}

6 Conclusions

The decay constants and spectrum of heavy-light mesons have been determined in the quenched approximation to lattice QCD, with comparison made to other determinations and experiment. A large value of the pseudoscalar decay constant is found, relative to other lattice determinations. This is due in part to the choice of quantity used to set the lattice scale. Different scale-setting choices are also responsible for the largest systematic error contribution in the results, reflecting an unavoidable uncertainty in quenched calculations. Results are compared at two values of the lattice spacing. The lack of agreement, and the failure of the data at $\beta = 6.0$ to satisfy heavy quark symmetry constraints suggest that $\mathcal{O}(a^2)$ discretisation errors are not small at the larger lattice spacing. At $\beta = 6.2$, the heavy quark symmetry constraints are well satisfied, suggesting that the main results are closer to the continuum limit, although distortion of the decay constants due to $\mathcal{O}(a^2)$ artefacts cannot be ruled out. It is worth noting that a continuum extrapolation has already been found necessary, when non-perturbative $\mathcal{O}(a)$ improvement is applied, even for light-quark quantities such as f_K [35]. Non-perturbative determinations of

the necessary improvement and renormalisation coefficients are used where available, but boosted perturbation theory values are taken for c_V and b_m. For c_V in particular, the large difference between the perturbative value used here and a preliminary non-perturbative determination would result in a significant change in the vector decay constants.

Acknowledgements

References

[1] M. Neubert and B. Stech, in *Heavy Flavours II*, Vol. 15 of *Advanced Series on High Energy Physics*, edited by A.J. Buras and M. Lindner (World Scientific, Singapore, 1998), Chap. 4, pp. 294–344.

[2] M. Ciuchini, R. Contino, E. Franco, and G. Martinelli, Eur. Phys. J. **C9**, 43 (1999).

[3] B. Sheikholeslami and R. Wohlert, Nucl. Phys. B **259**, 572 (1985).

[4] M. Lüscher, S. Sint, R. Sommer and P. Weisz, Nucl. Phys. B **478**, 365 (1996).

[5] M. Lüscher, S. Sint, R. Sommer, P. Weisz, H. Wittig and U. Wolff, Nucl. Phys. B (Proc. Suppl.) **53**, 905 (1997).

[6] M. Creutz, Phys. Rev. D **36**, 2394 (1987).

[7] F. Brown and T. Woch, Phys. Rev. Lett. **58**, 163 (1987).

[8] N. Cabibbo and E. Marinari, Phys. Lett. B **119**, 387 (1982).

[9] UKQCD Collaboration, K.C. Bowler *et al.*, To be published in Phys. Rev. D, hep-lat/9910022.

[10] B. Efron, SIAM Review **21**, 460 (1979).

[11] R. Sommer, Nucl. Phys. **B411**, 839 (1994).

[12] M. Guagnelli, R. Sommer and H. Wittig, Nucl. Phys. B **535**, 389 (1998).

[13] R. Sommer, Nucl. Phys. Proc. Suppl **60A**, 279 (1998).

[14] M. Guagnelli and R. Sommer, Nucl. Phys. B (Proc. Suppl.) **63A-C**, 886 (1998).

[15] T. Bhattacharya *et al.*, Phys. Lett. B **461**, 79 (1999).

[16] T. Bhattacharya, R. Gupta, W. Lee, S. Sharpe, Nucl. Phys. B (Proc. Suppl.) **83-84**, 851 (2000).

[17] S. Sint and P. Weisz, Nucl. Phys. B **502**, 251 (1997).

[18] G.M. de Divitiis and R. Petronzio, Phys. Lett. B **419**, 311 (1998).

[19] M. Lüscher, S. Sint, R. Sommer, and H. Wittig, Nucl. Phys. B **491**, 344 (1997).

[20] P. Boyle, hep-lat/9903033.

[21] M. Neubert, Phys. Rev. D **45**, 2451 (1992).

[22] M. Neubert, Phys. Rev. D **46**, 1076 (1992).

[23] S. Bethke, Nucl. Phys. B (Proc. Suppl.) **54A**, 314 (1997).

[24] T. Draper, Nucl. Phys. B (Proc. Suppl.) **73**, 43 (1999).

[25] S. Hashimoto, Nucl. Phys. B (Proc. Suppl.) **83-84**, 1 (2000).

[26] A.X. El-Khadra, A.S. Kronfeld, and P.B. Mackenzie, Phys. Rev. D **55**, 587 (1997).

[27] D. Becirevic *et al.*, Phys. Rev. D **60**, 074501 (1999).

[28] C. Bernard *et al.*, Phys. Rev. Lett. **81**, 4812 (1998).

[29] CP-PACS Collaboration, A. Ali Khan *et al.*, Nucl. Phys. B (Proc. Suppl.) **83-84**, 331 (2000).

[30] UKQCD Collaboration, D.G. Richards, Nucl. Phys. B (Proc. Suppl.) **73**, 381 (1999).

[31] UKQCD Collaboration, V.I. Lesk *et al.*, Nucl. Phys. B (Proc. Suppl.) **83-84**, 313 (2000).

[32] L. Lellouch and C.J.D. Lin, hep-ph/9912322.

[33] F. Muheim, private communication.

[34] C. Caso *et al.*, Eur. Phys. J. C **3**, 1 (1998).

[35] J. Garden, J. Heitger, R. Sommer and H. Wittig, Nucl. Phys. B **571**, 237 (2000).